Research Article Vol. 33, No. 7 / 7 Apr 2025 / Optics Express 15603
Optics EXPRESS

20 µm-core polarization maintaining endlessly single mode photonic crystal fiber for delivery of high-power single frequency lasers

S. VIDAL,[1,*] L. GIBERT,[1] M. ZAMBELLI,[1] T. RATEL,[1] M. BERISSET,[1] L. PROVINO,[2] A. MONTEVILLE,[2] R. POUYET,[2] O. LE GOFFIC,[2] S. CLAUDOT,[2] T. CHARTIER,[3] C. PIERRE,[1] AND M. CASTAING[1]

[1]*ALPhANOV, Centre Technologique Optique et Laser, Rue François Mitterrand, F-33400 Talence, France*
[2]*Photonics Bretagne, 4 rue Louis de Broglie, F-22300 Lannion, France*
[3]*Institut Foton, CNRS UMR 6082, Université de Rennes, F-22300 Lannion, France*
[*]*sebastien.vidal@alphanov.com*

Abstract: We report on the development of a 20 µm-core polarization maintaining endlessly single-mode photonic crystal fiber for use in the delivery of high-power single-frequency lasers, especially for quantum physics experiments. A complete numerical study is used to determine the optimal geometry of the fiber to be single mode over the 600-1700nm spectral range with a polarization extinction ratio greater than 20 dB. Three versions of this fiber with different pitch and hole size ratios were fabricated and experimentally characterized at 780 nm, 1064 nm, and 1550 nm. The Brillouin threshold was also measured at 1064 nm and compared to that obtained with commercial fibers.

1. Introduction

Since the appearance of the so-called endlessly single-mode fiber in the late 1990s, photonic crystal fibers (PCFs) and the exploration of the great variety of possible applications have attracted particular attention [1,2]. They have been successfully used in many fields such as optical communications [3], supercontinuum generation [4] or high-power fiber laser [5]. This is also an excellent solution for quantum applications [6]. Moreover, polarization maintaining (PM) PCFs maintain single-mode transmission of high-power, low noise single frequency lasers used for trapping and atoms cooling while keeping the initial linear polarization state. PM behavior was first introduced into a fiber by careful positioning of capillaries with the same external diameter but different wall thicknesses, leading to different airhole sizes in the cladding of the final fiber and twofold rotational symmetry [7]. Another approach then consisted of applying stress parts outside the cladding region [8]. Since the realization of the first PM PCFs, having mode field diameters from about 4 to 6.5 micron, with stress rods in 2004 [8], the development of this type of fiber is increasingly controlled. NKT Photonics (now part of Hamamatsu) is notably one of the world leaders in the supply of PCFs with a high degree of maturity with their ''LMA-PM-xx'' fiber series, the LMA-PM-15 being the reference for high power delivery with its core diameter of 15 µm [9]. At the same time, the enthusiasm for quantum physics, which requires more and more power, is motivating the development of increasingly powerful single-frequency low-noise laser sources around 1 µm [10,11] and in the visible via non-linear conversion [12]. With the emergence of these high-power sources which can deliver several hundred watts, current fibers are a limitation for beam delivery because the threshold of stimulated Brillouin scattering will be reached [13]. To give an order of magnitude and based on the theory presented in [13], the threshold is of the order of 12 W at 1064 nm for a 10m-long LMA-PM-15 fiber.

In this paper, we present the development of a 20 µm-core polarization maintaining PCF particularly suitable for delivering higher power. Based on a complete numerical study, we

#544176 https://doi.org/10.1364/OE.544176
Journal © 2025 Received 16 Oct 2024; revised 25 Feb 2025; accepted 4 Mar 2025; published 1 Apr 2025

Optics EXPRESS

determine the optimal geometry of the fiber. Three versions of this fiber with different pitch and holes size ratios were fabricated and experimentally characterized at 780 nm, 1064 nm and 1550 nm. We measured a Brillouin threshold of around 25 W at 1064 for a 10m-long section, which justifies the interest of this fiber compared to existing fibers. We also verified the transport of more than 40W at 1064 nm with a 5m-long fiber without distortion.

2. Numerical study

2.1. Choosing the geometry to simulate

Among the large existing design families, we chose a design composed of a solid central area surrounded by a microstructured area incorporating air holes arranged in hexagonal symmetry. We also inserted two stress zones on either side of the central zone at the periphery of the microstructures (see Fig. 1). The number of rows of holes is set to 4, in the same way as the structure presented in [8]. This is a good compromise between feasibility and the targeted level of birefringence (by bringing the stress bars closer to the core of the structure). This will also allow to have a reasonable outside diameter.

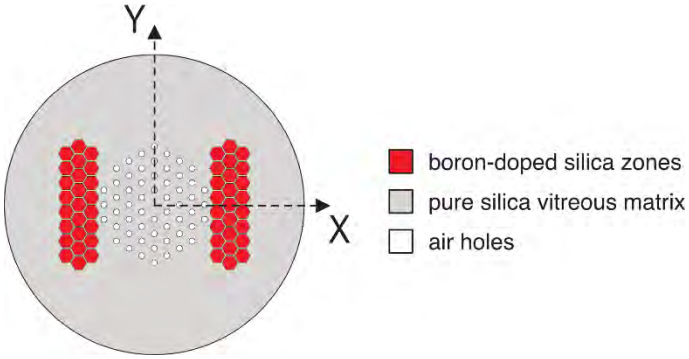

Fig. 1. Cross-section sketched of the 20-µm core polarization maintaining PCF.

The core diameter D of the fiber, chosen equal to 20 µm, is defined as $D = \Lambda \cdot (2 - d/\Lambda)$, where d is the diameter of the air holes and Λ the spacing between the air holes, called pitch. The guiding properties as a function of the geometrical parameters were simulated by first calculating, using a commercial finite element software, the stress distribution due to the presence of boron rods by applying the plane-strain approximation. Based on this, the refractive index change resulting from the elasto-optical effect was evaluated in the fiber cross-section. Then, a complex full-vector modal solver, based on the finite element method and utilizing conformal mapping and perfectly matched layers, was applied to calculate the effective index and losses of the guided modes in both the straight and bent fiber. Material dispersion was also taken into consideration.

2.2. Geometry optimization

The loss evolution of the higher-order mode LP_{11}-like was simulated as a function of d/Λ in the 600-1100 nm spectral range (see Fig. 2).

Using the monodicity criterion, a fiber based on this geometry will be single-mode over the 600-1700nm spectral-range for $d/\Lambda \leq 0.43$ because the losses of higher order modes are greater than 10 dB/m over this range.

We also simulated the bending sensitivity, which is an important parameter for the final use of the fiber. The evolution of the average losses of the X and Y-polarized fundamental modes as a function of the bending radius was studied at 1 µm wavelength for different values of the d/Λ

Optics EXPRESS

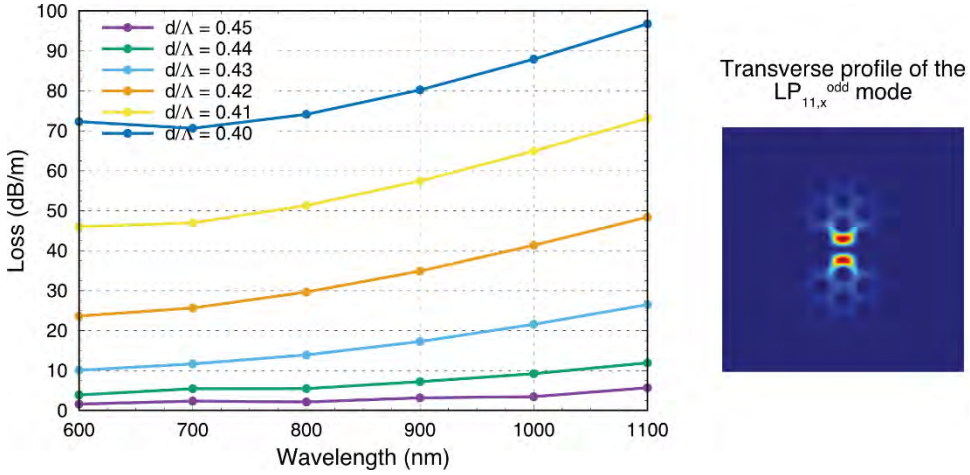

Fig. 2. Loss evolution of the higher-order mode with the lowest losses ($LP_{11,\,x}^{\,odd}$) as a function of d/Λ in the 600-1100 nm spectral range (left). Transverse profile of the $LP_{11,\,x}^{\,odd}$ mode, the mode image represents the z-component of the Poynting vector at 1064 nm of the LP_{11} mode leaking into the microstructure. (right).

ratio (see Fig. 3). The least bend sensitive fiber design appears to be obtained for $d/\Lambda = 0.43$. Indeed, for a radius of curvature greater than 11 cm, the losses of the fundamental mode remain less than 0.1 dB/m.

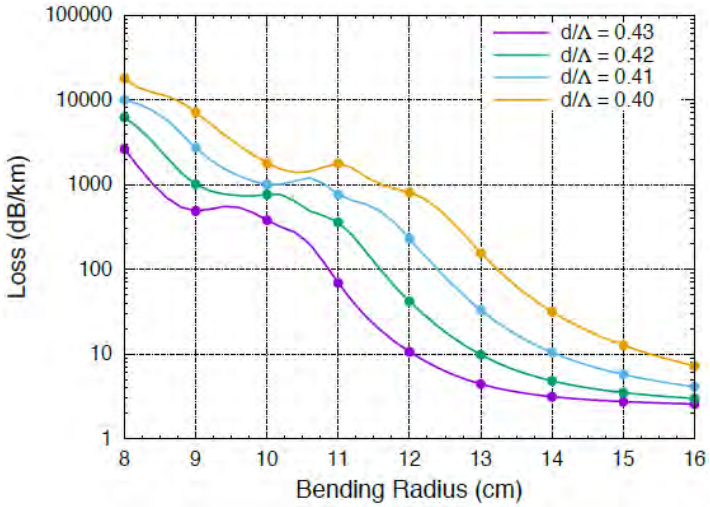

Fig. 3. Evolution of the average losses of the X and Y-polarized fundamental modes as a function of the bending radius at 1 µm for different values of the d/Λ ratio.

We then evaluated the fundamental mode field diameter (MFD) of the X and Y-polarized fundamental modes and the phase birefringence curve from 600 nm to 1.7 µm for different values of d/Λ ratio. The results obtained for example for $d/\Lambda = 0.43$ are shown in Fig. 4. We observe that the MFD values are almost constant around 17 µm and that the phase birefringence is greater than 1.3×10^{-4}. Results are essentially the same for different d/Λ ratios.

Optics EXPRESS

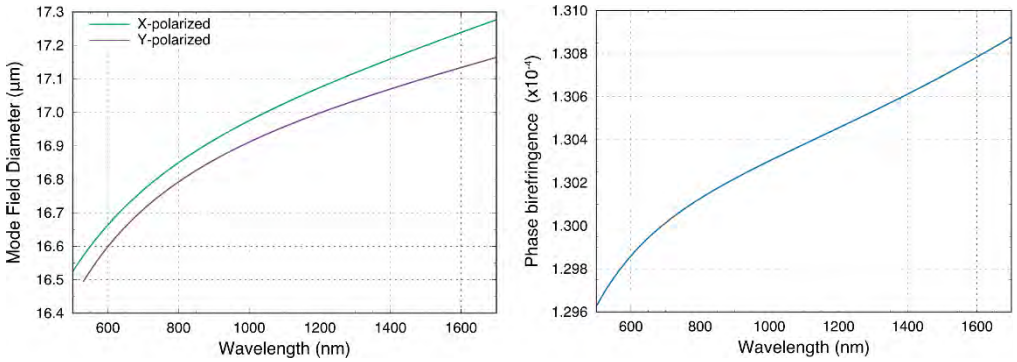

Fig. 4. Evolution of the MFD of the X and Y-polarized fundamental modes (left) and the phase birefringence curve (right) for $d/\Lambda = 0.43$.

3. Experimental characterization

PM-PCFs with three d/Λ ratios (0.41, 0.43 and 0.45) were fabricated using the stack-and-draw method [14], and drawing to optical fiber at Photonics Bretagne. A microscope image of the realized 20 µm-core and 260 µm-clad PM-PCF structure is shown in Fig. 5, where we can observe the 4 rows of holes and the two stress zones on either side of the central zone at the periphery of the microstructures.

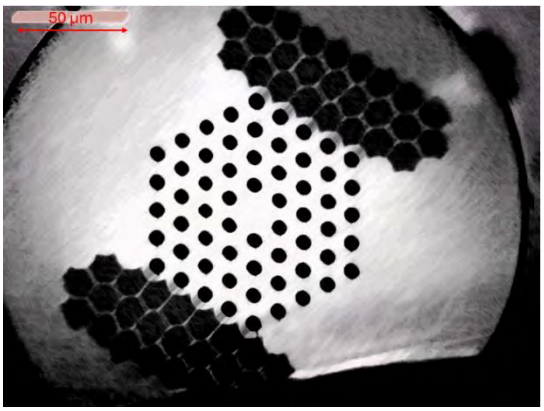

Fig. 5. Microscope image of the 20µm-core and 260µm-clad PM-PCF fabricated.

3.1. Full characterization at 1064 nm

First, we measured the phase birefringence for the three versions of this fiber using the magneto-optical method with 6m-long sections. To do these measurements, we used a DFB laser at 1064 nm and a magnet that can be translated along the longitudinal direction of the fiber producing an axial magnetic field. The principle of this method is described in [15]. We measured for all three fibers the same order of magnitude for phase birefringence, $1.15 \times 10^{-4} \pm 2 \times 10^{-6}$, only 11% lower than the expected theoretical value (see Table 1).

We measured the losses by making cutbacks with a delta length from 295 to 75 meters of fiber bent on a 32 cm diameter spool. The average values for the 3 batches of fiber are 31 dB/km.

Then, we measured the polarization extinction ratio (PER) of these three fibers using the cross-polarizer method (CPM) [16]. This technique requires a broadband source. Light emitted

Optics EXPRESS

Table 1. Phase birefringence, M^2 and PER measurements at 1064 nm for the three d/Λ ratios of PM-PCF fiber.

Fiber	Phase birefringence	M^2 (x/y)	PER (dB)
PM-PCF $d/\Lambda = 0.41$	$1.16 \times 10^{-4} \pm 2 \times 10^{-6}$	1.12 / 1.12	28 ± 1
PM-PCF $d/\Lambda = 0.43$	$1.15 \times 10^{-4} \pm 2 \times 10^{-6}$	1.09 / 1.08	30 ± 1
PM-PCF $d/\Lambda = 0.45$	$1.15 \times 10^{-4} \pm 2 \times 10^{-6}$	1.05 / 1.10	26 ± 1

from an ASE source is first polarized with the help of a polarizing beam splitter cube. The resulting PER is measured with a commercial device (ERM200 - Benchtop Extinction Ratio Meter, 600 nm - 1600 nm from Thorlabs), it is of the order of 30 dB (device resolution limit). Light is then injected into the core of our PCF fibers using a pair of adapted lenses, a half wave plate being inserted to align the polarization axis along one of the two fiber axes. We measured the PER with our commercial device for the three d/Λ ratios and each time on 5m-long and 30 m-long fiber sections. Fibers are coiled on the optical table with a bending radius of 15 cm. We obtained very good PER output from the fibers, regardless of the length of the sections, always greater than 26 dB and even approaching 30 dB for $d/\Lambda = 0.43$ (see Table 1). PER measurement over 10 hours shows variations of less than 0.7 dB compared to the average value. We obtain the same results by injecting along the two birefringence axes of the fibers.

We then evaluated the modal quality of these fibers as well as the threshold for the appearance of the Brillouin effect. We used a single-frequency laser source delivering 60 W at 1064 nm. It is composed of a commercial seeder delivering 20 mW with a spectral linewidth < 30 kHz (Koheras ADJUSTIK from NKT Photonics) followed by three homemade fiber amplifiers. The output of the last amplifier stage, composed of a DC-200/40-PZ-Yb active fiber from NKT Photonics, is collimated with a beam diameter of 2 mm at $1/e^2$. A "λ/2 – beam splitter cube" assembly then allows the incident power to be adjusted without modifying beam propagation parameters and a free space isolator is used to isolate the laser but also to recover in reflection the Brillouin power which will be backscattered. Then two mirrors and a lens of adapted focal length are used to optimize the injection into the different fibers to be tested. We studied the modal behavior of the three versions of the PM-PCF fiber on the 5m-long and 30m-long sections studied previously and we measured $M^2 < 1.12$ each time (see Table 1). An example of spatial profile and M^2 measurement for a 30m-long PM-PCF fiber with $d/\Lambda = 0.43$ are shown in Fig. 6.

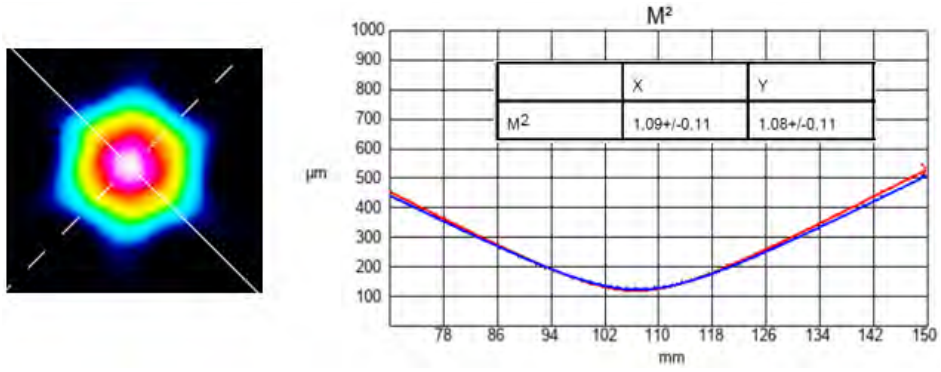

Fig. 6. Spatial profile (left) and M^2 measurement at 1064 nm (right) for a 30m-long PM-PCF fiber with a $d/\Lambda = 0.43$.

Table 1 summarizes the measurements obtained for the three PM-PCF fiber architectures. The results are very good for all three versions of the fiber.

Optics EXPRESS

We finally evaluated the Brillouin threshold of these fibers using the backscattered power reflected by the optical isolator. Estimating the Brillouin threshold of an optical fiber requires measuring the transmitted and backscattered powers as a function of the injected power, this is called a power diagram. Knowledge of the power injected is essential in determining the Brillouin threshold. To evaluate the coupling efficiency, we inject a low power signal to be in linear regime and we add the linear losses of the fiber to the output power, values provided by industrial partners. We also added the Fresnel losses induced by the exit face. In the power diagrams, we define the Brillouin threshold power as the input power for which the backscattered power reaches 1% of the input pump power [17,18]. The input face of the tested fibers is cleaved at 8° and a high index polymer is placed over several centimeters to evacuate the uncoupled power.

We first validated our experimental device by carrying out the measurement on the well-known PM980 fiber on a 10 m-long section. When the polarization axis of the incident wave is aligned along one of the two birefringence axes of the fiber, we measure a threshold power of $P_{exp} = 3.55$ W (see Fig. 7). Theoretically, we can estimate this value using the following formula [13]:

$$P_{th} = \frac{21.K.A_{eff}}{L_{eff}.g_B}, \tag{1}$$

where K is a quantity linked to the polarization of the incident and Stokes waves ($K = 1$ for PM fiber), $A_{eff} = \pi MFD^2 / 4$ is the effective area, L_{eff} is the effective length and g_B corresponds to the Brillouin gain of a monochromatic wave ($g_B = 2 \times 10^{-11}$ m/W in silica at 1064 nm). The effective length is defined as $L_{eff} = (1 - e^{-\alpha L}) / \alpha$ with L the fiber length (10 m in our case) and α the linear loss of the fiber. Using $\alpha = 2.5$ dB/km and $MFD = 7$ µm [19], we obtain $P_{th} \approx 4$W. We observe a very good agreement between the theoretical and experimental values, noting that there are obviously uncertainties on both values, linked to the measurement for P_{exp} and to the uncertainty on the MFD for the theoretical value, but we estimate an order of magnitude. Note that when the incident light was polarized at 45° to the fiber axis, we measure a Brillouin threshold power twice that obtained when the light was aligned, in agreement with [20].

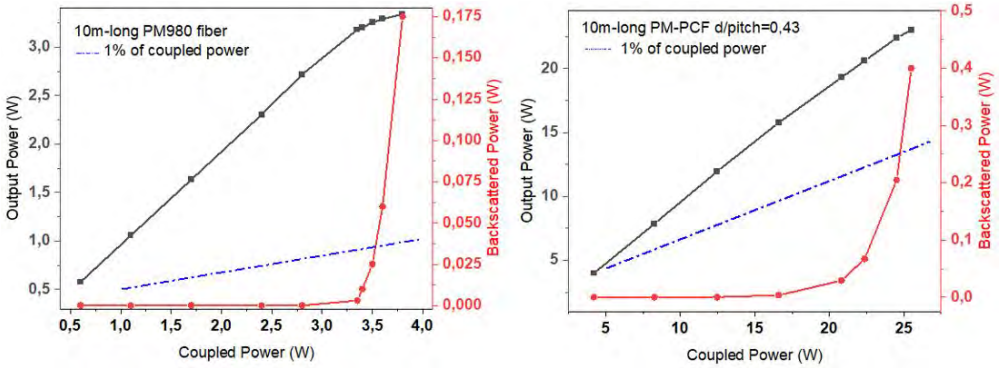

Fig. 7. Measurement of the power diagram for a 10m-long PM980 (left), used to qualify the setup, and for the 10m-long PM-PCF with $d/\Lambda = 0.43$ (right). The transmitted powers are represented by square dots and the backscattered powers by circle dots. The dotted lines represent 1% of the coupled power.

Once our setup was qualified, we then measured the Brillouin threshold for the three versions of the PM-PCF fiber (on 10m-long sections) as well as for the three fibers of the ''LMA-PM-xx'' series marketed by NKT Photonics [9], called LMA-PM-5, LMA-PM-10 and LMA-PM-15, again on 10m-long sections. We chose 10m-long sections for all fibers to be able to access the

Optics EXPRESS

Brillouin threshold with the available laser power and to be able to easily compare the results. We can observe for example in Fig. 7 the power diagram obtained for the PM-PCF fiber with $d/\Lambda = 0.43$, the threshold power being close to 25 W.

All experimental results and the data used to determine the associated theoretical values are presented in Table 2. For all these measurements, the polarization axis of the incident wave is aligned with one of the birefringence axes of the fibers (we obtain the same result along both axes). We observe good agreement between experimental results (column 4) and those obtained from formula (1) (column 5). This means that this formula, determined for all-silica fibers, can also be used with this type of PCF fibers. It has been shown in the past that this is not always true, particularly for PCF fibers with a small core, which have a higher Brillouin threshold than that predicted by theory [21]. Following our observations, we can therefore exploit formula (1) to approximately determine the value of the Brillouin threshold as a function of the length of the fiber and thus choose the fiber best suited to the desired application. Note that, to the best of our knowledge, this is the first time that an experimental measurement of the Brillouin threshold of LMA-PM-xx fibers from NKT Photonics has been carried out and compared to theory.

Table 2. Experimental Brillouin threshold power at 1064 nm for the 10m-long tested fibers and associated theoretical values. The values of MFD and α are given by the suppliers and are used to determine theoretical values.

Fiber	MFD (µm)	α (dB/km)	P_{exp} (W)	P_{th} (W)
PM980 [18]	(7.0 ± 0.5)	<2.5	3.55	$3.5 < P_{th} < 4.7$
LMA-PM-5 [8]	(4.4 ± 0.5)	<7	1.50	$1.2 < P_{th} < 2.0$
LMA-PM-10 [8]	(8.6 ± 0.5)	<5	4.20	$5.2 < P_{th} < 6.9$
LMA-PM-15 [8]	(12.6 ± 1.5)	<10	9.10	$10.2 < P_{th} < 14.0$
PM-PCF $d/\Lambda = 0.41$	(17.0 ± 1.5)	<30	17.50	$20.0 < P_{th} < 28.5$
PM-PCF $d/\Lambda = 0.43$	(17.0 ± 1.5)	<30	25	$20.0 < P_{th} < 28.5$
PM-PCF $d/\Lambda = 0.45$	(17.0 ± 1.5)	<30	20	$20.0 < P_{th} < 28.5$

In Table 2, the fiber with $d/\Lambda = 0.43$ shows a higher threshold but it is difficult to say whether it is the d/Λ ratio that has an influence on this value because a very slight variation of the MFD can also quickly influence the threshold value. To better understand these observations, we measured the MFD of the three PCF fibers and we indeed observed that the one with $d/\Lambda = 0.43$ had a slightly higher MFD (17 µm) than the other two, MFD = 16.4 µm for $d/\Lambda = 0.41$ and 16.8 µm for $d/\Lambda = 0.45$.

Figure 8 represents the evolution of P_{exp} with the MFD and we observe a quadratic evolution, as predicted by (1), which means that the small variation of d/Λ has no influence at this stage. This is not to say that there is not a particular architecture that would increase the threshold value because a recent study on the development of Brillouin laser has demonstrated that the Brillouin gain coefficient could be improved by changing the geometric structural parameters of PCF fibers [22]. A more systematic and in-depth study would be necessary to determine whether another architecture still allows this threshold to be moved further away.

To conclude, it clearly appears that our 20 µm-core PM-PCF fiber is of definite interest for delivery of high-power single-frequency laser because it has a much higher Brillouin threshold. Indeed, we delivered 40 W in a 5m-long fiber with $d/\Lambda = 0.43$ without any distortion.

3.2. Characterization at 780 nm and 1550 nm

To verify the endlessly single mode behavior of our fiber, we also performed characterizations at 780 nm and 1550 nm. 780 nm is a wavelength that is widely exploited for cooling Rubidium atoms, the most common atomic species used for making alkali gas Bose-Einstein condensates [23,24]. The wavelength of 1550 nm is also very useful in quantum physics to create dipole traps

Optics EXPRESS

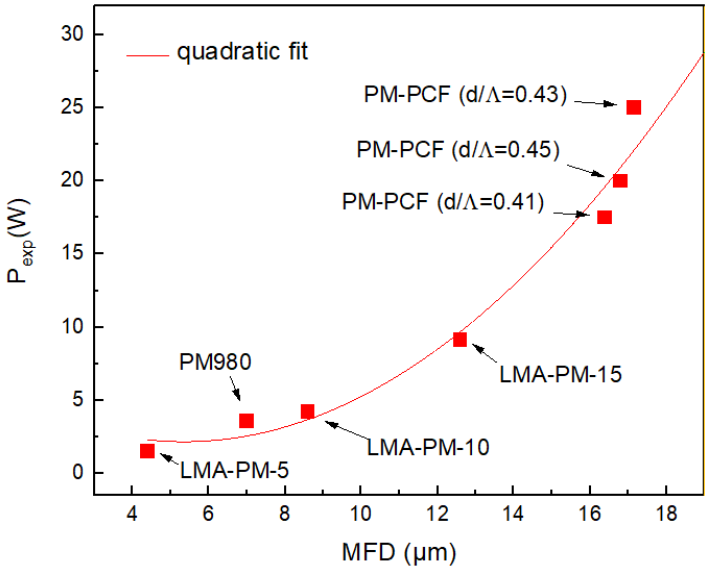

Fig. 8. Experimental Brillouin threshold power at 1064 nm for the 10m-long tested fiber

[25] and for optical communications [26]. It is therefore a serious advantage to have an endlessly single-mode fiber capable of delivering high optical power in these spectral ranges.

At 780 nm, we used a super-luminescent diode from Thorlabs delivering 5.5 mW with a spectral bandwidth of 18 nm at half-maximum. We started by checking that the transmission was very good (greater than 70%, depending on the quality of the free space injection). Then, we studied the modal behavior of the three versions of the PM-PCF fiber on the 5m-long and 30m-long sections previously studied and we measured $M^2 < 1.12$ each time (see Table 3). An example of spatial profile and M^2 measurement for a 5m-long PM-PCF fiber with $d/\Lambda = 0.43$ are shown in Fig. 9.

Table 3. M^2 and PER measurements at 780 nm and 1550 nm for the three d/Λ ratios of PM-PCF fiber.

	780nm		1550 nm	
Fiber	M^2 (x/y)	PER (dB)	M^2 (x/y)	PER (dB)
PM-PCF $d/\Lambda = 0.41$	1.07 / 1.12	28 ± 1	1.08/ 1.10	30 ± 1
PM-PCF $d/\Lambda = 0.43$	1.08 / 1.11	29 ± 1	1.09/ 1.09	30 ± 1
PM-PCF $d/\Lambda = 0.45$	1.08/ 1.08	29 ± 1	1.10/ 1.08	30 ± 1

Then, we measured the PER of these three fibers using the cross-polarizer method. The experimental device is the same as those used at 1064 nm, we just replaced the optics to make them suitable for this wavelength. We obtained very good PER output from the fibers, regardless of the length of the sections, always greater than 28 dB (see Table 3).

At this wavelength (as at 1550 nm), we do not have a single frequency source powerful enough to measure the threshold of the Brillouin effect. However, we have shown at 1064 nm that (1) allows us to predict the threshold of the appearance for this kind of PM-PCFs. We can therefore use (1) to extrapolate the Brillouin threshold to other wavelengths, we will thus have access to a significant order of magnitude. In Eq. (1), the Brillouin gain g_B is the main factor that evolves

Optics EXPRESS

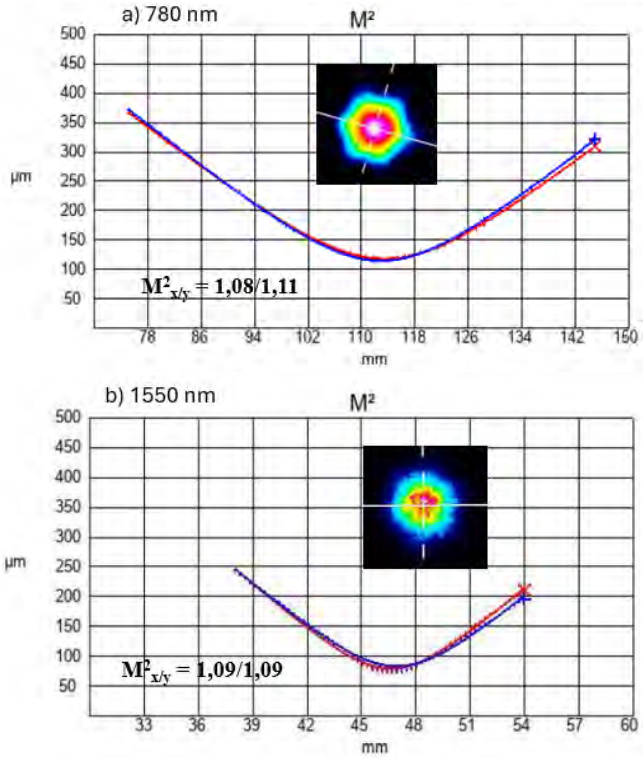

Fig. 9. Spatial profile (inset) and M^2 measurement at 780 nm (a)) and 1550 nm b)) for a 5m-long PM-PCF fiber with a d/Λ ratio = 0.43.

with the wavelength λ, g_B being proportional to $1/\lambda^2$ [13]. The slight variation of α with λ must also be considered.

We finally carried out the same type of measurement at 1550 nm using an ASE source. An example of spatial profile and M^2 measurement for a 5m-long PM-PCF fiber with $d/\Lambda = 0.43$ are shown in Fig. 9(b)). We used a WinCamD-LCM camera from DataRay (with the 1.5 µm extension) which has a limited resolution explaining the slightly pixelated appearance of the mode. Complete results are presented in Table 3. Once again, we obtained very good PER output from the fibers, always around 30 dB.

We also measured losses at these two wavelengths, the average values for the 3 batches of fiber being respectively 64 dB/km at 780 nm and 16 dB/km at 1560 nm.

4. Conclusion

We presented the development of a 20 µm-core polarization maintaining endlessly single mode photonic crystal fiber for the use in delivery of high-power single frequency lasers required for the quantum field. Based on an in-depth numerical study, three versions of this fiber with different pitch and holes size ratios were drawn. We have fully characterized these three versions of the fiber at 1064 nm by measuring transmission, phase birefringence, PER and modal quality. We also measured the threshold of appearance of the Brillouin effect at 1064 nm which is the first non-linear effect limiting the delivering power in single frequency regime. We have shown that our fiber has a much higher threshold than existing commercial fibers and we demonstrated the transport of more than 40 W at 1064 nm with a 5m-long fiber without distortion. Thanks to our study, we proved that the theory existing for all-silica fibers could describe the behavior of

Optics EXPRESS

large-core PCF fibers and that we could therefore extrapolate our results to other wavelengths. We thus have access to a database allowing us to choose the PM-PCF fiber best suited to the desired experience.

Additional measurements at 780 nm and 1550 nm demonstrated endlessly single mode behavior as well as the conservation of PER. We observed very good results for all three versions of the fiber. At this stage, it is difficult to choose one rather than another although the fiber with $d/\Lambda = 0.43$ seems to present slightly better results, especially due to a slightly higher MFD.

We are currently working on the functionalization of this 20µm-core fiber including end-cap splicing, sheating and high-power connectors with mode striper and heat sink to make this fiber robust and easily usable. We can also add anti-reflective coatings at the interfaces to increase the transmission efficiency of these cables.

Funding. Conseil Régional Nouvelle Aquitaine; Conseil Régional de Bretagne.

Acknowledgment. We thank Valérian Freysz and Maëlys Rigouleau for the development of the software allowing the measurement of PER.

The Conseil Regional Nouvelle Aquitaine is greatly acknowledged for financial support.

This work was supported by Région Bretagne, Département Côtes-d'Armor, and Lannion Trégor Communauté

Disclosures. S. Vidal, L. Gibert, M. Zambelli, T. Ratel, M. Berisset, C. Pierre and M. Castaing: ALPhANOV, F-33400 Talence, France (E). L. Provino, A. Monteville, R. Pouyet, O. Le Goffic, S. Claudot, Photonics Bretagne, F-22300 Lannion, France (E).

The authors declare there are no other conflicts of interest.

Data availability. Data underlying the results presented in this paper are not publicly available at this time but may be obtained from the authors upon reasonable request.

References

1. T. A. Birks, J. C. Knight, and P. S. J. Russell, "Endlessly single-mode photonic crystal fiber," Opt. Lett. **22**(13), 961–963 (1997).
2. J. C. Knight, "Photonic crystal fibres," Nature **424**(6950), 847–851 (2003).
3. H. Ademgil and S. Haxha, "Design and Optimisation of Photonic Crystal Fibres for Applications in Communication Systems," *Proceedings of the World Congress on Engineering* 425–428 (2007).
4. W. J. Wadsworth, N. Joly, J. C. Knight, *et al.*, "Supercontinuum and four-wave mixing with Q-switched pulses in endlessly single-mode photonic crystal fibres," Opt. Express **12**(2), 299–309 (2004).
5. J. Limpert, T. Schreiber, S. Nolte, *et al.*, "High-power air-clad large-mode-area photonic crystal fiber laser," Opt. Express **11**(7), 818–823 (2003).
6. J. G. Rarity, J. Fulconis, J. Duligall, *et al.*, "Photonic crystal fiber source of correlated photon pairs," Opt. Express **13**(2), 534–544 (2005).
7. A. Ortigosa-Blanch, J. C. Knight, W. J. Wadsworth, *et al.*, "Highly birefringent photonic crystal fibers," Opt. Lett. **25**(18), 1325–1327 (2000).
8. R. Folkenberg, M. D. Nielsen, N. A. Mortensen, *et al.*, "Polarization maintaining large mode area photonic crystal fiber," Opt. Express **12**(5), 956–960 (2004).
9. NKT Photonics, https://www.nktphotonics.com/products/optical-fibers-and-modules/large-mode-area-photonic-crystal-fibers-polarization-maintaining/.
10. C. Dixneuf, G. Guiraud, Y.-V. Bardin, *et al.*, "Ultra-low intensity noise, all fiber 365 W linearly polarized single frequency laser at 1064 nm," Opt. Express **28**(8), 10960–10969 (2020).
11. C. Shi, S. Fu, X. Deng, *et al.*, "435 W single-frequency all-fiber amplifier at 1064 nm based on cascaded hybrid active fibers," Opt. Commun. **502**, 127428 (2022).
12. C.-H. Feng, S. Vidal, P. Robert, *et al.*, "High power continuous laser at 461 nm based on a compact and high-efficiency frequency-doubling linear cavity," Opt. Express **29**(17), 27760–27767 (2021).
13. E. P. Ippen and R. H. Stolen, "Stimulated Brillouin scattering in optical fibers," Appl. Phys. Lett. **21**(11), 539–541 (1972).
14. T. Y. Cho, G. H. Kim, K. Lee, *et al.*, "Study on the Fabrication Process of Polarization Maintaining Photonic Crystal Fibers and Their Optical Properties," J. Opt. Soc. Korea **12**(1), 19–24 (2008).
15. T. Chartier, C. Greverie, and L. Selle, "Ludovic Carlus, Grégory Bouquet, Louis-Anne de Montmorillo, "Measurement of the stress-optic coefficient of single-mode fibers using a magneto-optic method"," Opt. Express **11**(20), 2561–2566 (2003).
16. TIA 455-193, "Polarization crosstalk test method for polarization- maintaining optical fibers," USA, 2013.
17. P. Bayvel and P. M. Radmore, "Solutions of the SBS equations in single mode optical fibers and implications for fiber transmission systems," Electron. Lett. **26**(7), 434–436 (1990).
18. J.-C. Beugnot, T. Sylvestre, D. Alasia, *et al.*, "Complete experimental characterization of stimulated Brillouin scattering in photonic crystal fiber," Opt. Express **15**(23), 15517–15522 (2007).

Optics EXPRESS

19. Thorlabs, https://www.thorlabs.com/thorproduct.cfm?partnumber=PM980-XP.
20. R. H. Stolen, "Polarization effects in fiber Raman and Brillouin lasers," IEEE J. Quantum Electron. **15**(10), 1157–1160 (1979).
21. P. Dainese, P. S. J. Russel, N. Joly, *et al.*, "Stimulated Brillouin scattering from multi-GHz-guided acoustic phonons in nanostructured photonic crystal fibres," Nat. Phys. **2**(6), 388–392 (2006).
22. C. Liu, N. Song, F. Gao, *et al.*, "Polarization-maintaining photonic crystal fiber with high Brillouin gain coefficient for Brillouin lasers," Appl. Opt. **62**(26), 6892–6898 (2023).
23. M. H. Anderson, J. R. Ensher, M. R. Matthews, *et al.*, "Observation of Bose-Einstein Condensation in a Dilute Atomic Vapor," Science **269**(5221), 198–201 (1995).
24. H. Ludvigsen, A. Xijala, A. Pietilainen, *et al.*, "Laser Cooling of Rubidium Atoms in a Vapor Cell," Phys. Scr. **49**(4), 424–428 (1994).
25. Y.-J. Lin, A. R. Perry, R. L. Compton, *et al.*, "Rapid production of ^{87}Rb Bose-Einstein condensates in a combined magnetic and optical potential," Phys. Rev. A **79**(6), 063631 (2009).
26. D. J. Richardson, J. M. Fini, and L. E. Nelson, "Space-division multiplexing in optical fibres," Nat. Photonics **7**(5), 354–362 (2013).